High Voltage Supply for a CubeSat Sized Hall Effect Thruster

DTU Space

BSc Thesis

Julie Søborg Dresler Petersen
June 2017

DTU Space
National Space Institute

Prepared by

Julie Søborg Dresler Petersen (s144126)

Supervised by

René Fléron, Arnold Knott & Frederik Monrad Spliid

Bachelor's Thesis - Earth and Space Physics and Engineering

Technical University of Denmark

9th of June 2017

Abstract

Electrical propulsion is ideal for CubeSat propulsion as it is very efficient, it does not take up a lot of space and can run off the electrical power supply, that is already powering the remaining parts of the satellite. To power a Hall Effect thruster, one of the most well know electrical propulsion systems, a high voltage supply is needed. Hence the power from the EPS on the satellite will have to undergo a conversion to a higher voltage.

This thesis comes up with a design for a high voltage converter, that can be used to drive the Hall Effect Thruster. For the design the flyback topology has been selected since it takes advantage of the turns ratio in the coupled inductor to further boost the voltage. The design has been build and tested to a certain extent. To ensure that it works, however further tests and development will be necessary before it is mounted on a satellite.

Resumé

Elektrostatisk fremdrift er ideelt at benytte til at drive en CubeSat, da det ikke optager megen plads, har en høj virkningsgrad og kan drives af den strømforsyning der allerede leverer strøm til de andre systemer på satelliten. Til at drive en Hall effekt ionmotor, en af de mest benyttede elektrostatiske motorer, er man nødt til at have en høj spænding. Den spænding som forsyningen leverer må altså transformeres til en højere spænding.

Dette projekt fremstiller et løsningforslag til hvordan denne højspændingsomformer kan konstrueres, så den er kraftig nok til at drive en Hall effekt ionmotor. Flyback topologion er blevet valgt til omformeren, da den drager nytte af viklingsforholdet i den koblede spole til yderligere at øge spændingen. Løsningsforslaget er blevet bygget og testet til en hvis grad for at sikre at det virker, yderligere forsøg og udvikling er dog nødvendigt før det kan monteres på en satellit.

Preface

This thesis has been written to meet the demands for obtaining a Bachelor of Science degree in Earth and Space Physics and Engineering from the Technical University.

The thesis project has been carried out at the National Space Institute, with assistance from the Power Electronics Group at the Department of Electrical Engineering.
The thesis contents represents 15 ECTS

The thesis work has been carried out in the period from March 2017 to June 2017

I would like to grasp this opportunity to thank my supervisors René Fléron, Arnold Knott and Frederik Monrad Spliid for their counseling, ideas and support throughout the project. Furthermore I would like to thank the students at the Power Electronics department. Without their help and greater knowledge within electronics, I would not have been able to complete the thesis in time. I would especially like to thank family and friends for my supporting me during this period.

Contents

1 Preamble

Humanity has always yearned for new horizons, as has so often been proved throughout history where Christopher Columbus and James Cook may be mentioned as some of the greatest and most well know explorers on Earth. But not only planet Earth has brought up an lust for exploration in mankind, also what lies beyond has fascinated many for thousands of years. Along with the Industrial Revolution and the Information Age, the possibility of space exploration became a reality instead of just a dream.
From launching the first spacecraft, to building an international space station, the technology has advanced immensely. Things may look nothing like the fictional spacecrafts and -stations in films, but they are advancing and improving every day.
The space exploration continues, and to keep making progress, new methods must be created. If mankind ever wish to study the deep space, faster and more efficient probes are needed, than the ones existing today.

To make faster probes, one must look at the propulsion system. So far chemical propulsion has dominated, it is however very inefficient, as it gives a large acceleration but in a very short amount of time. One must therefore look beyond this propulsion type and towards other possibilities.
Electrical propulsion may be one of the options for a solution, since it can be made more efficient with a small acceleration, over a longer amount of time. One of the most famous types of electrical propulsion is the Hall effect thruster, which uses ionized gas that collides with electrons as the thrust force.

This report concerns the design and building process of a flyback converter, to create a high voltage supply for a CubeSat sized Hall effect thruster. It states the frame of reference as an opening, before moving on to the design process of the circuit and collecting results, whereafter it terminates in a discussion of the errors.

2 Frame of reference

2.1 The supply system

The power supply on the satellite charges energy from solar arrays into a series of batteries, which then delivers power to the remaining part of the satellite. A numerous amount of subsystems are working within the satellite, among these a communication system which draws a great amount of power from the supply, which leaves little for the remaining subsystems. The system properties may be found in section 3.

2.2 Hall effect thruster

In 1879 Edwin Hall discovered the Hall effect. An effect that builds on the physical principles of electrostatics, and which states that when a current along a semiconductor is exposed to a perpendicular magnetic field, a voltage can be measured in the other direction. [1] The effect is used in the Hall effect thruster, where an ionized gas is fed through an anode, into a radial magnetic field, which then accelerates the gas outwards of the thruster, where it is met by electrons from a cathode. The ions and electrons collide, and create a force, which can be used as propulsion. [2] A simple illustration of the thruster can be seen on figure 1.

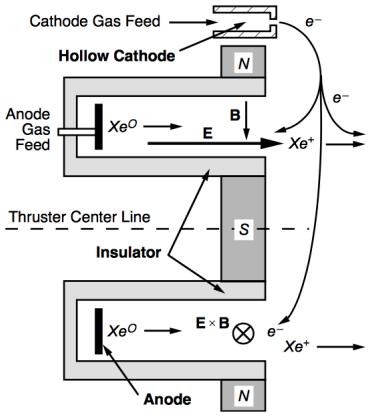

Figure 1: Illustration of a simple Hall effect thruster [2]

The Hall effect thruster may not be the most powerful kind of thruster, as the acceleration is very low. It is however very energy efficient, which makes it ideal for long journeys, as the acceleration does not matter as much here. The thruster has also been used for attitude control systems on satellites, to keep them in place.

A high power supply system is needed to induce an electric field, which creates the Hall Effect that accelerates the gas towards the magnetic field.

Equation 2.1 shows how the specific impulse is directly proportional with the input voltage, whereas a higher voltage will give more thrust. In the equation η_m is the mass utilization efficiency and M_a is the ion mass.

$$Isp = 1.417 \cdot 10^3 \gamma \eta_m \sqrt{\frac{V_b}{M_a}} \tag{2.1}$$

The specific impulse determines the thrust force, from equation 2.2, where g_0 is the acceleration at the Earth's surface, and $\dot{m}$ is the mass flow.

$$F = Isp \cdot \dot{m} \cdot g_0 \tag{2.2}$$

2.3 Issues

Due to the low supply power to the high voltage converter system, it is not possible to obtain a constant high power. The converter is created in a way where it converts the low input voltage to a high voltage, however at low currents. To obtain a high output power, the constant voltage must be cut into pulses, so charge can accumulate in a capacitor until the desires power level is reached.
This creates some problems when working with a thruster fed with gas, as the gas will leak from the thruster, without adding to the acceleration, while the capacitor is charging. This makes this kind of power supply very inefficient for a propulsion system such as this.

2.4 Solutions

2.4.1 Field emission electric propulsion

The Field Emission Electric Propulsion or FEEP thruster takes its offspring in electrostatics as well, however instead of using ionized gas, liquid metal is used. Charge is applied and a Taylor cone is shaped from the liquid metal, whereas ions are accelerated from the tip, to create propulsion. The efficiency of this kind of propulsion is very high, however the minimum power needed to supply the system is a great deal higher than for the Hall Effect thruster. As to whether this kind of electrical propulsion system would work whilst being supplied by pulses may be difficult to determine as well, since the liquid metal will have to form a new Taylor cone and exhaust ions at each pulse. [3]

2.4.2 Pulsed plasma thruster

A Pulsed Plasma Thruster or PPT resembles a Hall effect thruster in many ways, but instead of using a gas which might leak, a solid propellant is used. A small spark has the purpose of turning a little bit of the surface of the propellant into a plasma, whereafter it will go through the same process as the Hall effect thruster. As propellant is exhausted, a spring will move the remaining forwards towards the ignition spark.

Since this kind of proportion is already pulsed at the output, a pulsed power supply will not make a great difference. The acceleration will not be as high, but it will still be just as efficient, as if it was powered by a constant power source, since the solid propellant will not leak. Furthermore, the PPT requires a lower power input, so it can be run more often, due to the shorter capacitor charge time. [5]
Teflon is most often used as propellant in the PPT, as it has a low friction coefficient, and very little outgassing properties in vacuum, which means that almost no material is lost during the off periods of the thruster.

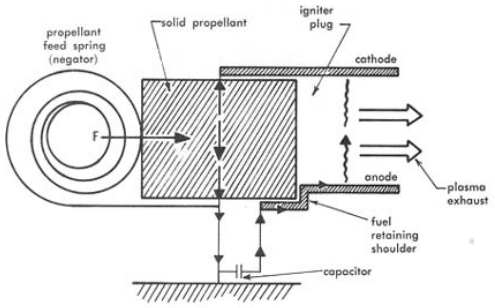

Figure 2: Illustration of a simple pulsed plasma thruster [4]

2.5 The mission goal

The future in space exploration has a need for more efficient propulsion systems than the chemical ones in use on today's spacecrafts. As science evolves, and the curiosity of mankind grows larger, greater goals are set. From the first satellite in space, to landing a man on the moon, and to sending space probes out past Pluto, the goals have evolved. However, to be able to achieve the next generation of goals within a lifetime, the propulsion must be more efficient.
The power supply created in this project is a step along the way, to advance the propulsion systems, and to be able to go further into space. This first draft may not be able to achieve any goals, it may however inspire to continue improving.

2.5.1 Asteroid mining

As the whole space industry is evolving, so is the spectrum of ideas. One of the newer concepts is asteroid mining, where Near Earth Asteroids are the main target, as they are closer to Earth, than for instance, the Asteroids in the Asteroid Belt between Mars and Jupiter. Asteroids contain many valuable resources, such as metals but also hydrogen and oxygen. The metals can be mined and either brought down to Earth, where the rare ones, in particular the platinum-group metals can be sold for a high prize and used in the industry, or be processed in space and used to further develop the space industry.
Extracting the resources from the asteroids is however not easy, and several different mining solutions has been proposed by the two main private asteroid mining companies, Deep Space Industries and Planetary Resources. All the solutions rely on small satellite scouts, that travel to the asteroid, and wiil closer determine what materials the asteroid is made of. For this process, CubeSats running off electric propulsion will be ideal, as they are small, so numerous can be sent into space at once, and they are energy efficient so they are able to travel far to track down the asteroids.
Asteroid mining will help lower the cost of space exploration, as all materials do not have to be brought out into space, which will result in larger funds for other space programs. [6]

3 System properties

To get an overview of the power balances, table 1 and 2 is set up, where the DC-DC converter and pulse generator parameters are displayed, respectively. Lower and upper limits are set for the parameters, if they are available and relevant.

DC-DC converter		
Parameter	**Lower limit**	**Upper limit**
Supply voltage	3.3 V	-
Supply current	0.15 A	1.5 A
Supply power	-	0.5 W
Output voltage	0.5 kV	1.0 kV
Output current	-	0.5 mA
Output power	-	0.5 W

Table 1: System properties table

On table 1 the properties for the DC-DC converter is shown. The supplied voltage and current is drawn from the on board electric power system on the satellite, and are therefore fixed. 1.5 A can be drawn from the supply at a short amount of time, but over longer periods the power must not exceed 0.5 W. The output values are the values desired to run the Hall effect thruster, which is being designed for the satellite.
It is worth to note, that it is assumed that the converter is ideal in the calculations of the output current and power.

$$P_{in} = P_{out} \tag{3.1}$$

This will not be the case for the actual converter, but it gives a good picture of how the output values will be compared to the input.
Table 2 shows the values for the pulse generator. Due to the low input power, the current is reduced a lot in the transformer, to create a higher voltage. Since the required output power is 1 kW, pulses must be made to accumulate charge in a capacitor, and then discharge it all at once in a pulse.

To determine the pulse frequency, the capacitor size must be found by equation 3.2, where the output is in Joule. [7]

$$W = \frac{1}{2}CV^2 \tag{3.2}$$

Since Watt is Joule per second, a pulse of 10 μs will require a 20 nF capacitor. Is this capacitor put in series with a load resistance of 20 MΩ the waiting time between the pulses will be 2 s, as shown in equation 3.3, which makes the frequency 500 mHz, which is calculated in equation 3.4.

$$t = 5RC = 5 \cdot 20\,\mathrm{M\Omega} \cdot 20\,\mathrm{nF} = 2\,\mathrm{s} \tag{3.3}$$

Pulse generator		
Parameter	**Lower limit**	**Upper limit**
Supply voltage	0.5 kV	1.0 kV
Supply current	-	0.5 mA
Supply power	-	0.5 W
Output voltage	500 V	1000 V
Output current	-	1 A
Output power	-	1.0 kW
Pulse frequency	-	500 mHz
Pulse width	-	2 μs

Table 2: System properties table

$$f_{pulse} = \frac{1}{2\,\mathrm{s} + 10\,\mu\mathrm{s}} = 500\,\mathrm{mHz} \tag{3.4}$$

A frequency of 500 mHz is very slow, so the Hall effect thruster will suffer under the charge time, as discussed in section 2.3. A smaller load will lower the time, but it must however still be able to withstand the high voltage coming from the converter without shorting.

4 Fundamental theory

To convert a voltage to either a lower or higher level, a DC-DC converter is needed. They all consists of a switch, and a type of inductor in which power can be stored and released. To obtain a larger voltage the most common converter is the boost converter. The boost converter is able to transform the voltage in accordance with equation 4.1, in which d, the duty cycle, is the percentage of time the switch is at the on state in the circuit.

$$V_{out} = V_{in}\frac{1}{1-d} \tag{4.1}$$

To get this to convert the voltage from 3.3 V to 1 kV, it would have to run at a 99.67 % duty cycle, which is very unrealistic to make.

To obtain a larger voltage, one can take advantage of the turns ratio of transformer or a coupled inductor, instead of using a standard single inductor.
The flyback converter uses the coupled inductor to store energy, and transform the voltage at the same time, which makes it ideal as the solution to this project.

4.1 The flyback converter

The flyback converter builds on the principles of the buck-boost converter, which is shown on figure 3. The buck-boost uses an inductor to store energy when a switch is closed, which is then released once the switch is opened.
When the switch is closed, current will pass through it, and into the inductor, where it will charge the core. This is shown by the red path on figure 3. When the switch then is open, the green path on figure 3 is followed, due to the stored current in the core, and an output voltage of V_o is present. Because of the direction of the current through the inductor, displayed by i_L, the output voltage will have the opposite polarity compared to the input voltage.

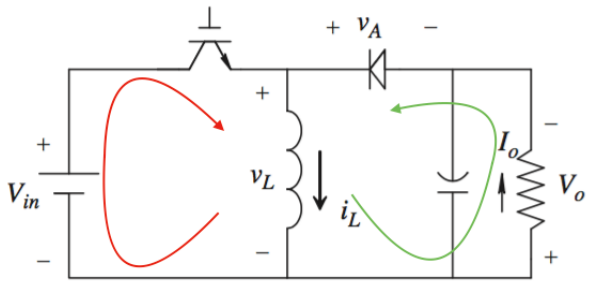

Figure 3: Schematic of a buck-boost converter

The flyback converter uses the same principles as the buck-boost converter, however instead of a single inductor, a coupled inductor is used, to achieve higher output voltages, due to the turns ratio in the coupled inductor.
The flyback converter consists of a DC power source, V_{in}, which is going to be supplied by the solar panels, which then charges the battery on the satellite. It then needs a switch, where most often a

MOSFET is used. The switch controls the current in the circuit.

Instead of using a transformer, a coupled inductor is used, since it can store energy in the core. The relationship between the inductances can be described by

$$\frac{L_1}{L_2} = \left(\frac{N_1}{k\,N_2}\right)^2 \tag{4.2}$$

where N_i is the amount of turns on the coil. The polarity of the coils are different, to achieve a positive output voltage.

On figure 4 the red path on the figure, shows the path when the switch is closed. Current will be stored in the core of the coupled inductor, since the diode blocks the current from running through the capacitor and resistor. The block is due to a voltage less than 0 between the diode and the capacitor, and since the voltage drop across the capacitor goes downwards, the voltage at the bottom of the capacitor must be 0. The voltage drop of the secondary winding is positive due to the polarity, whereas the voltage at the top of the secondary winding must be above 0. This means that the diode blocks, since the voltage is positive on the right side of it, and negative on the left side of it, and it can not have a negative forward voltage drop.

The green path shows the path of the current when the switch is open. The energy from the coil is released out into the circuit where it passes through the diode and creates an output voltage of V_o. The

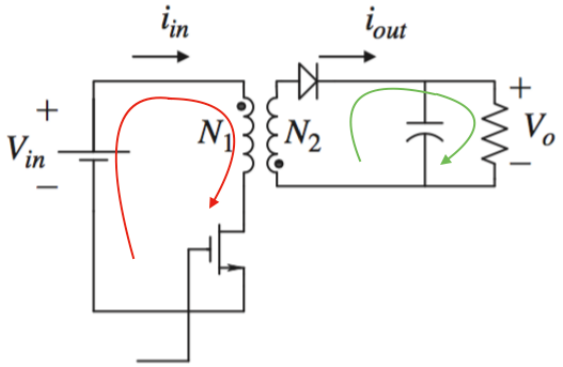

Figure 4: Schematic of a flyback converter

transfer function for a flyback converter is shown in equation 4.3, where d is the duty cycle, and N_i the amount of turns on the primary and secondary windings.

$$\frac{V_{out}}{V_{in}} = \frac{N_2}{N_1}\frac{d}{1-d} \tag{4.3}$$

Unlike the transfer function for the boost converter (equation 4.1) there is a turns ratio of the transformer who can help step up the voltage even more.

5 The design process of the DC-DC converter

To design the converter, a few parameters must be determined.
By looking at the transfer function (equation 4.3), one can see that the output voltage relationship is determined by the turns ratio and duty cycle. To keep the turns ratio a bit down, a higher duty cycle may be chosen. If the duty cycle is set to 50 % the turns ration is 1:303 whereas if a duty cycle of 70 % is chosen, the turns ratio only have to be 1:130. This makes a very large difference when constructing the coupled inductor.
Furthermore, the switching frequency of a flyback converter should be around 100-300 kHz, where a switching frequency in between is chosen, which is 200 kHz. This switching frequency produce a period of 5 μs as calculated from equation 5.1.

$$T_s = \frac{1}{f} = 5.0\mu\text{s} \tag{5.1}$$

5.1 Designing the coupled inductor

To design a coupled inductor, the core and wire parameters must be determined.[12] To do so, the magnetizing current is needed, and is found by equation 5.2.

$$I_M = \left(\frac{n_2}{n_1}\right)\frac{1}{d}\frac{V_{out}}{R_{load}} = 0.0928\,\text{A} \tag{5.2}$$

The magnetizing current ripple, Δi_M is set to be 20 %, which is fairly small since the magnetizing current itself is small. The maximum value is hence be found by equation 5.3.

$$I_{M,max} = I_M \cdot (\Delta i_M + 100\,\%) = 0.111\,\text{A} \tag{5.3}$$

From the magnetizing current (equation 5.2) the magnetizing inductance can be found. This is done by equation 5.4.

$$L_M = \frac{V_{in} d T_s}{2\Delta i_M} = 0.311\,\mu\text{H} \tag{5.4}$$

From the magnetizing current, the RMS values of the winding currents can be found, by using equation 5.5 for the primary winding, and equation 5.6 for the secondary winding. The results are as follows

$$I_{RMS,1} = I_M\sqrt{d}\sqrt{1 + \frac{1}{3}\left(\frac{\Delta i_M}{I_M}\right)^2} = 78.1\,\text{mA} \tag{5.5}$$

$$I_{RMS,2} = \frac{n_1}{n_2} I_M\sqrt{1-d}\sqrt{1 + \frac{1}{3}\left(\frac{\Delta i_M}{I_M}\right)^2} = 0.394\,\text{mA} \tag{5.6}$$

Whereas the total RMS current is given by equation 5.7 to be

$$I_{RMS,tot} = I_1 + \frac{n_2}{n_1} I_2 = 0.0.129\,\text{A} \tag{5.7}$$

From equation 5.3, 5.4 and 5.7 the physical parameters can be determined.

Since ETD cores were available at the institute, this kind of core is used. ETD is an acronym for Economic Transformer Design, and the core is made of Nickel-Zinc ferrite, which is suitable for higher

frequencies since it has a higher resistivity. Seven different core sizes where analyzed by the equations 5.8 and 5.9. [8]

$$n_1 = \frac{L_M I_{M,max}}{B_{max} A_c} 10^4 \tag{5.8}$$

$$n_2 = \left(\frac{n_2}{n_1}\right) n_1 \tag{5.9}$$

With an assumed maximum flux density of $B_{max} = 0.27$ T, the core with the best result was the ETD34 core, since it requires 15 windings on the primary side, and 1856 on the secondary side of the coupled inductor.

To determine the wire gauges, the fractions of the window area allocated to the primary and secondary windings can be determined by equation 5.10 and 5.11, which can then be used to find the wire gauges from equation 5.12 and 5.13.

$$\alpha_1 = \frac{I_1}{I_{tot}} = 0.604 \tag{5.10}$$

$$\alpha_2 = \frac{n_2 I_2}{n_1 I_{tot}} = 0.778 \tag{5.11}$$

With a desired window fill factor of 30 %, the wire gauges becomes

$$A_{W1} \leq \frac{\alpha_1 K_w W_A}{n_1} = 0.368\text{cm}^2 \tag{5.12}$$

$$A_{W2} \leq \frac{\alpha_2 K_w W_A}{n_2} = 0.00261\text{cm}^2 \tag{5.13}$$

The gauges reveals the cross sectional area of the wires, and from this the diameters of the wires can be determined by using equation 5.14, to be $D_{W1} \leq 0.65$ cm and $D_{W2} \leq 0.055$ cm.

$$D = 2\sqrt{\frac{A_W}{\pi}} \tag{5.14}$$

However, when operating with high frequencies, not all of the wire is used, and the wire might as well be hollow. The phenomenon is called the skin effect, and it can be calculated by equation 5.15. [9] For copper when the frequency is 200 kHz, the relative permeability is 0.999 and the resistivity is $1.678 \cdot 10^{-}8$ Ωm.

$$\delta = \sqrt{\frac{1}{\pi f \mu}} = 0.146\,\text{mm} \tag{5.15}$$

To make sure that all of the wire is used, a wire size of 0.2 mm is chosen. On the primary side however, where the wire should be significantly larger than this, parallel windings are made, to get the wanted size. Since the window had a length of 20.9 mm, 6 parallel wires can be used, per winding for the primary inductor.

When working with a long wire, the losses can be quite significant. Equation 5.16 is used to calculate the approximate copper losses, in the secondary winding, where they are most significant. [10]
To calculate the loss, the cross section area of the wire with a diameter of 0.2 mm, the length of one winding which appear of the data sheet to be 60.5 mm and the resistivity of copper of $2 \cdot 10^{-}8$ Wm is needed, along with the output current and the amount of windings. [11]

$$P_{Cu} = I^2 R = I^2 \frac{\rho_{Cu} n_2 l}{A} = 17.868\,\mathrm{mW} \tag{5.16}$$

Equation 5.16 reveals that the copper loss is 3.57 %, which is rather large, however unavoidable with this design.

5.2 Designing the switch

To do the switching, a MOSFET (metal–oxide–semiconductor field-effect transistor) and an IC to generate the signal for the MOSFET is chosen.
The supply voltage from the satellite power supply unit is only 3.3 V, so if this were to supply the switch, a logic level MOSFET would have to be used. So to simplify the design two 9 V batteries will be used to supply the MOSFET externally, as they will output 18 V when connected in series. This will have to be redesigned for the actual satellite, but it is efficient enough for testing. From the datasheet of the batteries [13] it is found that 550 mAh can be drawn from the battery. If we want the battery to work for 10 hours we then have 55 mA available. Setting this number a little lower, for 40 mA makes sure that the batteries last. This will also keep the temperature fairly low.
A n-channel MOSFET is used, since a p-channel MOSFET in this case will be a factor 3 worse.

5.2.1 Selecting the MOSFET

When selecting a proper MOSFET, the switching, conduction and gate driver losses must be taken into account.
The conduction losses can be found from equation 5.17 from the on-state resistance, the duty cycle and the RMS current [14].

$$P_{Mcl} = R_{DS(on)} d\, I_{RMS}^2 \tag{5.17}$$

The on-state resistance is dependent on the temperature, which in space will vary from around $-40°C$ to around $50°C$.
By examining equation 5.17 it appears that the relationship between the conduction loss and on-state resistance is directly proportional, whereas a low on-state resistance will cause lower losses.

The switching losses are calculated by using equation 5.18, where the rise and fall times associated with the MOSFET voltage and current, as well as the frequency and supply voltage are taken into consideration.

$$P_{Msw} = \frac{1}{2} V_{supply}\, I_{RMS}\, (t_{c,on} + t_{c,off})\, f_s \tag{5.18}$$

Again, the relationship is proportional between the losses and the rise and fall times, which varies from MOSFET to MOSFET.

The gate driver losses can be found from equation 5.19 which determines the average gate driver power loss, from the gate charge.

$$P_{Mgd} = f_{sw} \cdot Q_g \cdot V_g \tag{5.19}$$

The relationship in equation 5.19 is proportional as well, between the MOSFET parameter and loss.
From equation 5.17, 5.18 and 5.19 it is revealed that the on-state resistance, the rise and fall times, and the gate charge should all be as low as possible.

Besides the losses to consider, the drain-source voltage is also important to take into consideration.

This value should not be too large, so around 20 V would be fitting.

Taking all these things, and the stock status in consideration, the PHP55N03T [15] was selected, as it was on stock in the lab, had a drain-source voltage of 30 V, was easy to mount, and had a low on-resistance.

5.2.2 Selecting the IC

When selecting the gate driver IC, the supply voltage of 18 V, duty cycle of 70 % and the frequency of 200 kHz, must be taken into account. Furthermore the IC must be able to run with only an external power supply, and external resistors and capacitors, to avoid having to generate a signal for a gate driver.

5.2.3 First attempt: LT3748

The LT3748 IC from Linear Technologies [16] support these demands, and it is designed for flyback converters. The block diagram is displayed on figure 5, with all the ports and necessary external components. The resistor values for R_{FB} and R_{TC} can be found from equations given in the data sheet. The value of R_{REF} should according to the data sheet be 6040 Ω. R_{FB} can be found from equation 5.20 and R_{TC} from equation 5.21.

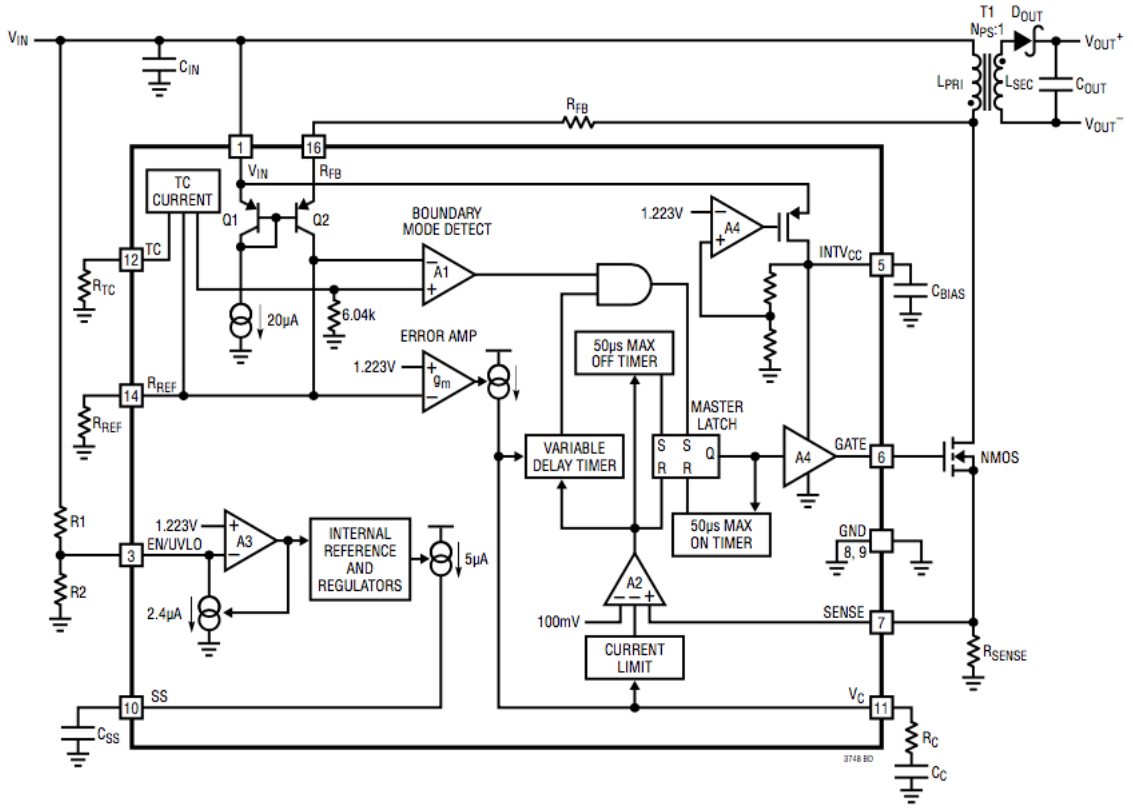

Figure 5: Block diagram of the LT3748 IC

$$R_{FB} = \frac{R_{REF} N_{PS}((V_{OUT} + V_F) + V_{TC})}{V_{BG}} \tag{5.20}$$

$$R_{TC} = \frac{R_{FB}}{N_{PS}} \frac{1.85\text{mV}/^\circ\text{C}}{\frac{\Delta V_{OUT}}{\Delta TEMP}} \tag{5.21}$$

Given in the datasheet for the IC, is the value for the bandgap reference of $V_{BG} = 1.223$ V, $V_{TC} = 0.55$ V and $\Delta TEMP = 1.85 \cdot 10^{-3}$ V/°C. Furthermore the forward voltage for the diode P600M is $V_f = 1$ V. The temperature difference is set to be the difference between the lower and upper limit of -55°C and 150°C respectively.

The values for the resistors $R1$ and $R2$ can be found by using voltage division (see equation 5.22). The input voltage at pin 3 must be 1.223 V according to the datasheet.

$$V_{pin3} = V_{in} \frac{R2}{R1 + R2} \tag{5.22}$$

For the sense resistor, equation 5.23 is used to estimate the value. Given in the data sheet is the value of $V_{sense} = 15 \cdot 10^{-3}$ and $t_{set} = 400 \cdot 10^{-9}$.

$$R_{sense} = \frac{V_{sense} \cdot L_{pri}}{N \cdot t_{set}(V_{out} + V_f)} \tag{5.23}$$

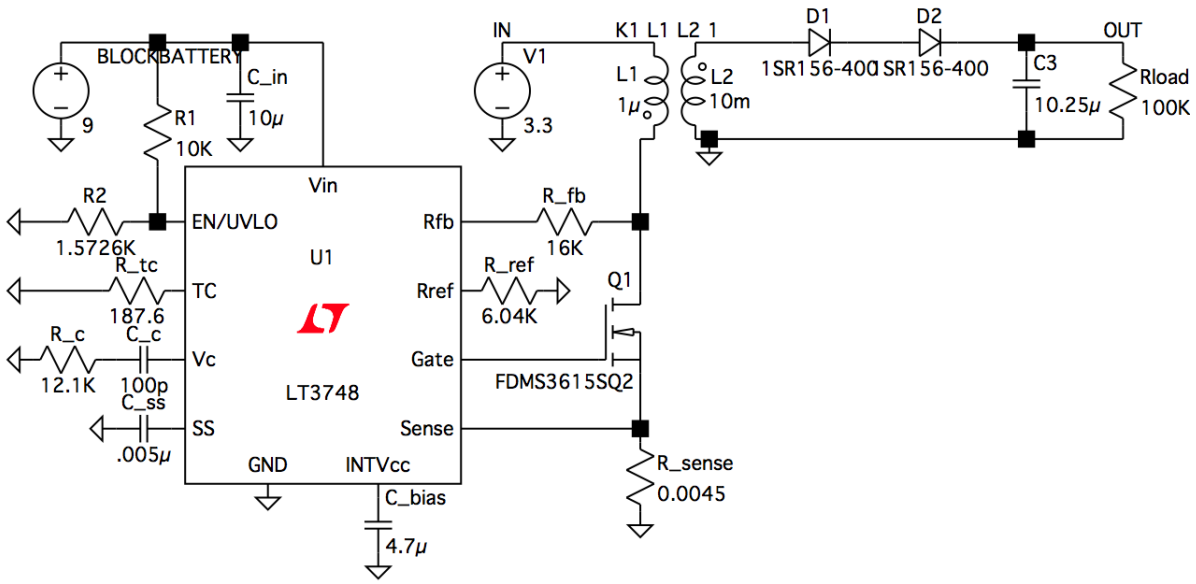

Figure 6: LT Spice simulation of the circuit using LT3748

On figure 6 an LT Spice simulation of the circuit with the IC is shown. The parameters for the coupled inductor, diodes, output capacitor and load is roughly estimated. The simulation is based on the data sheet for the IC and a demo circuit [17], where the capacitor values for the capacitors around the IC are kept at their original value.

Figure 7 shows the output voltage of the simulation, and it is clear that the output voltage won't go higher than about 13 V. The reason for this may be found in the signal from the switch, where it runs with

a duty cycle of close to 100 %, which barely allows the coupled inductor to discharge during the off-period.

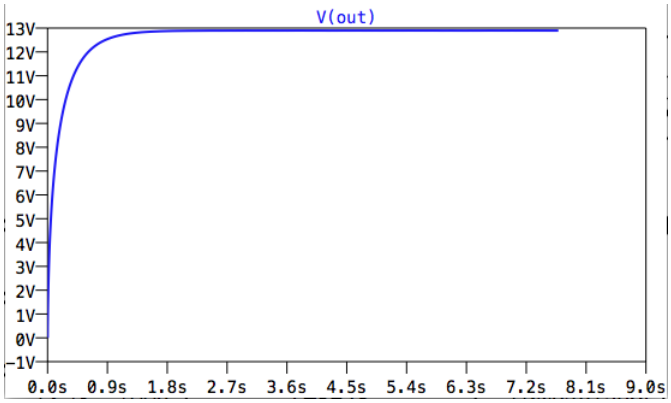

Figure 7: Output voltage waveform from the LT Spice simulation

This can be seen on figure 8, where there is zoomed in on the signal from the MOSFET to the coupled inductor. The duty cycle of this seems to be close to 100%.

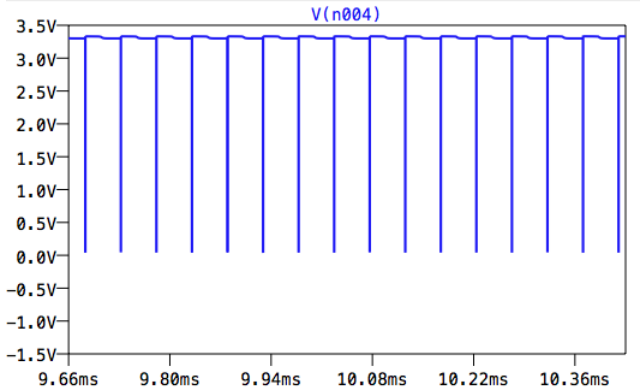

Figure 8: MOSFET output voltage waveform from the LT Spice simulation

The effect of this is shown on figure 9 where the two inductor currents are shown. The currents of the primary inductor is very large, and by far larger than what the EPS can handle.

There may be multiple reasons as to why this circuit did not work.
Some of the accompanying resistances or capacitors may have been at a wrong value, or connected incorrectly, making the duty cycle to large, and unable to drive the circuit.
It may have been unable to be driven from two different input voltages, of 3.3 V and 9 V, creating incoherence between the IC and the rest of the circuit.
With all the connections to be made between the external components to drive the IC, one of them could easily be wired incorrectly.
The turns ratio was to large for the IC to drive the circuit.

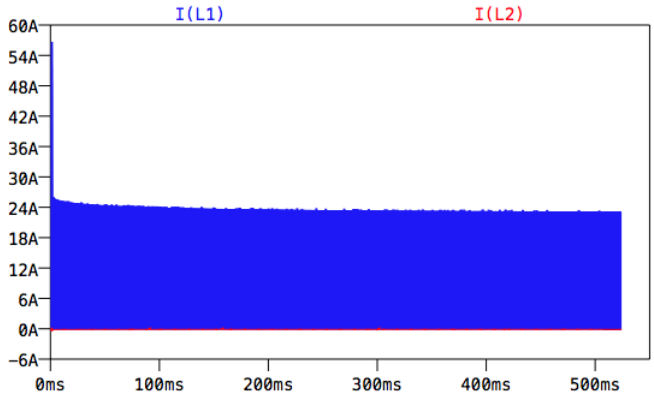

Figure 9: Inductor currents waveforms from the LT Spice simulation (primary,secondary)

5.2.4 Second attempt: UC3842B

Learning from the mistakes made with the first IC, the second IC choice fell on one more simple to connect to the circuit, the UC3842B IC [18]. From a more practical point of view it is also easier to wire, as it is larger and has less pins.

The block diagram of the IC is shown on figure 10, and compared to the first IC (block diagram on figure 5) it has fewer pins and external components, which makes it easier to connect and get running.

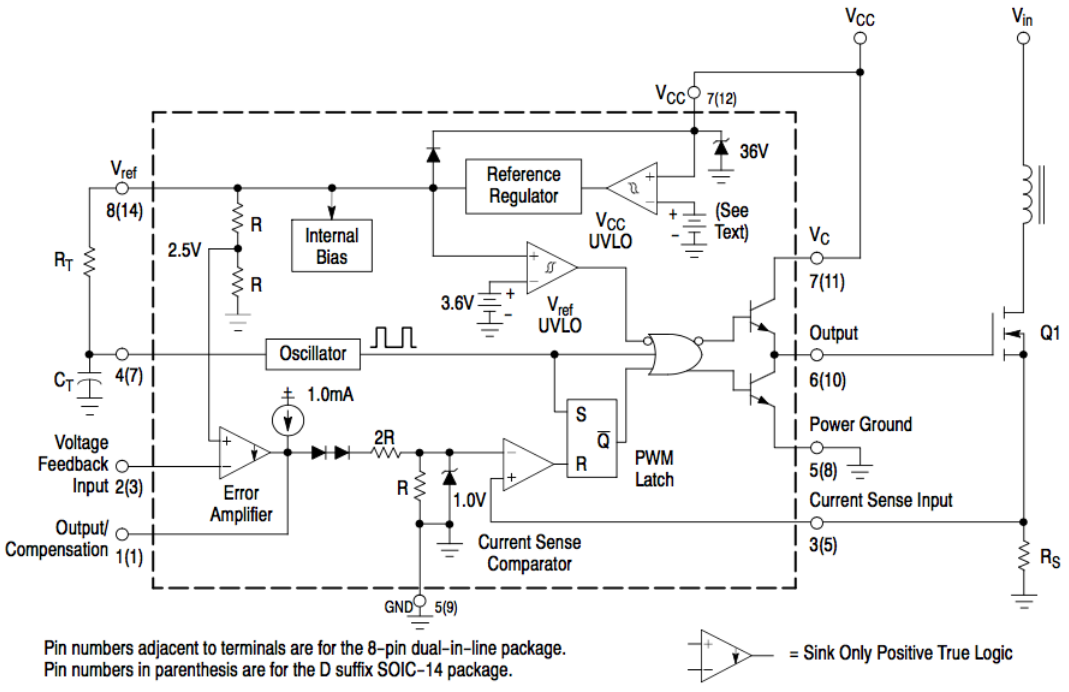

Figure 10: Block diagram of the UC3842B IC

The value of V_{CC} was at first lowered to 15 V by voltage division, to be able to use the predefined external resistor values. By measuring the voltage, it was discovered that the voltage was much lower than this, which was due to an inner resistance of the IC, which created a parallel resistance in the voltage division,

that lowered the voltage further. This was solved by switching the voltage division circuit to a voltage regulator of 15 V. However by further examining the data sheet, it was discovered that the threshold voltage should be at least 15 V for the IC to start, so the voltage regulation was neglected entirely.

The R_S (sense resistance) can be determined from equation 5.24, found in the data sheet. The maximum peak current was in section 3 mentioned to be 1.5 A, so the sense resistance must be 0.5 Ω.

$$I_{pk(max)} = \frac{1.0\,\mathrm{V}}{R_S} \tag{5.24}$$

The timing components, R_T and C_T can be determined by using the data sheet as well. Solving equation 5.25 reveals the resistance between pin 8 and 4. All values, except the duty cycle, is given in the data sheet, so one can easily determine R_T to be 1200 Ω.

$$d = \frac{\ln\left(\frac{V_{val}-V_{ref}}{V_{pk}-V_{ref}}\right)}{\ln\left(\frac{V_{val}-V_{ref}}{V_{pk}-V_{ref}} \cdot \frac{R_T \cdot I_{dis}+V_{pk}-V_{ref}}{R_T \cdot I_{dis}+V_{val}-V_{ref}}\right)} \tag{5.25}$$

From figure 2 in the data sheet, the C_T capacitance can be determined, from the timing resistor and the frequency to be 5 nF.

On figure 11 the switch test circuit is displayed. A capacitor has been connected between the input at pin 7, so the IC can draw power from this, and by that way draw power faster, than if it had to draw it directly from the batteries. A capacitor has also been connected at pin 8, for the same reason. To test the circuit, a load of 200 Ω has been mounted between the MOSFET and the input voltage source.

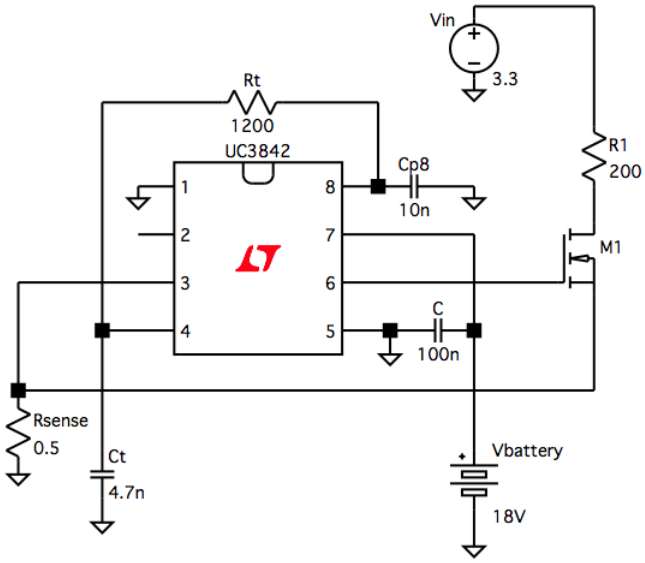

Figure 11: Schematic of the IC test circuit

Even though the circuit should work in theory, no signals were measured at the output. Voltages were measured by pin 8 and 4 though, so some signals must have been generated within the IC. Being unable to understand how to get it work, and after shorting 2 IC's, a decision was made to try something else. As the IC shorted, no data recording of the measurable voltages were made. Figure 12 shows a picture of the second version of the test circuit, before the IC shorted.

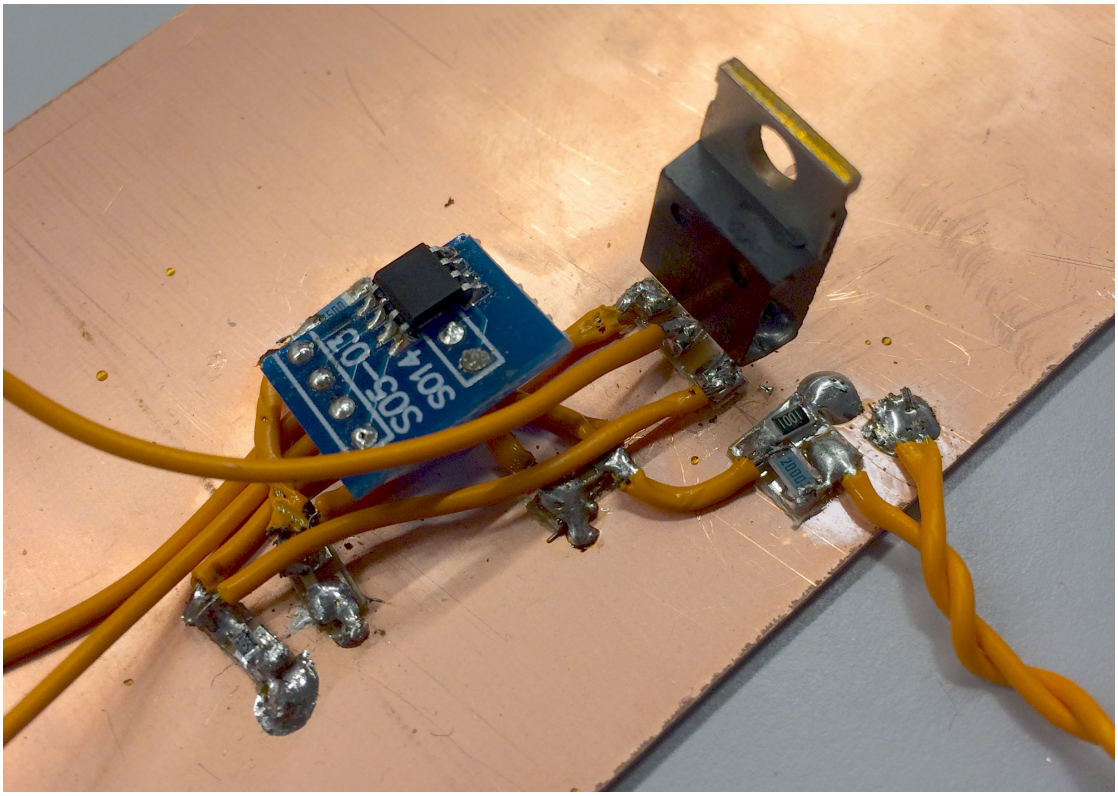

Figure 12: Picture of the IC test circuit

5.2.5 Third attempt: Astable Integrating Modulator

For the third attempt at creating a signal for the MOSFET, it was decided to discontinue the search for an IC to match the circuit demands, and instead build an Astable Integrating Modulator(AIM) to produce a regulating signal.[19]

An AIM consist of one or multiple comparators and a gate driver, accompanied by resistors and capacitors. The LT1016 comparator [20] will be used, as it meets the demands, and has the best ratings. The comparator will be powered with a 5 V supply voltage.

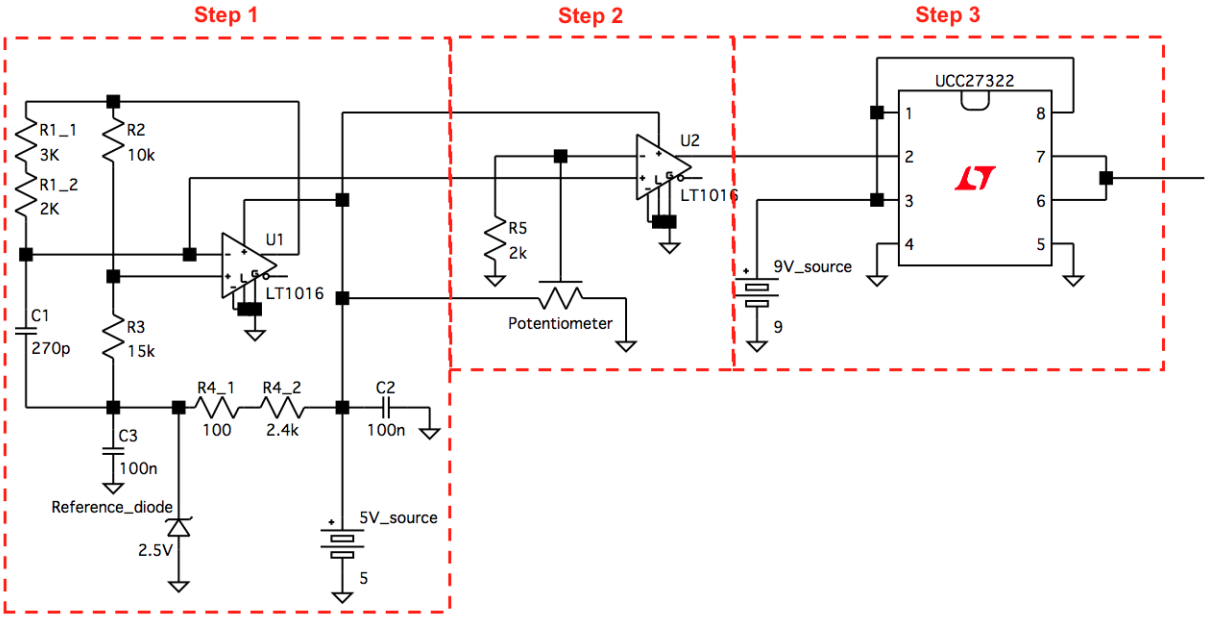

Figure 13: Schematic of the Astable Integrating Modulator

Figure 13 shows the AIM. It consists of three steps; step 1 creates a sawtooth waveform due to the capacitor, that is fed into step 2, which takes the signal and makes it square instead. Step 3 then enhances the signal from step 2, so it becomes strong enough to power a MOSFET.

Step 1

To get the comparator to work with the 5 V supply, 2.5 V must be applied to the inverting and non-inverting terminals. This is done by using the reference zener diode LM366 [21], and a 2.5 kΩ resistor, R4. R4 creates a voltages drop from 5 to 2.5 V, and the reference diode draws the excess current to maintain this voltage. 100 nF bypass capacitors has been connected at the supply, and at the reference diode so power can be drawn from the capacitors instead of from the supply, to make the voltages more stable. The resistor values for R1-R3 are given by another student who previously designed this circuit. The same applies to the value of C1, where the value determines the frequency.

The voltage at the inverting and non-inverting terminals can be analyzed. If the voltage output signal start in the high state (5 V), C1 will be charged exponentially, until the voltage at the inverting terminal crosses the voltage at the non-inverting terminal. The comparator then switches the output to low, as the inverting terminal voltage is higher. This cause the capacitor to discharge exponentially, until the voltages at the terminals again cross, whereas the output will switch back to high. This process repeats, and it is what is seen on figure 14.

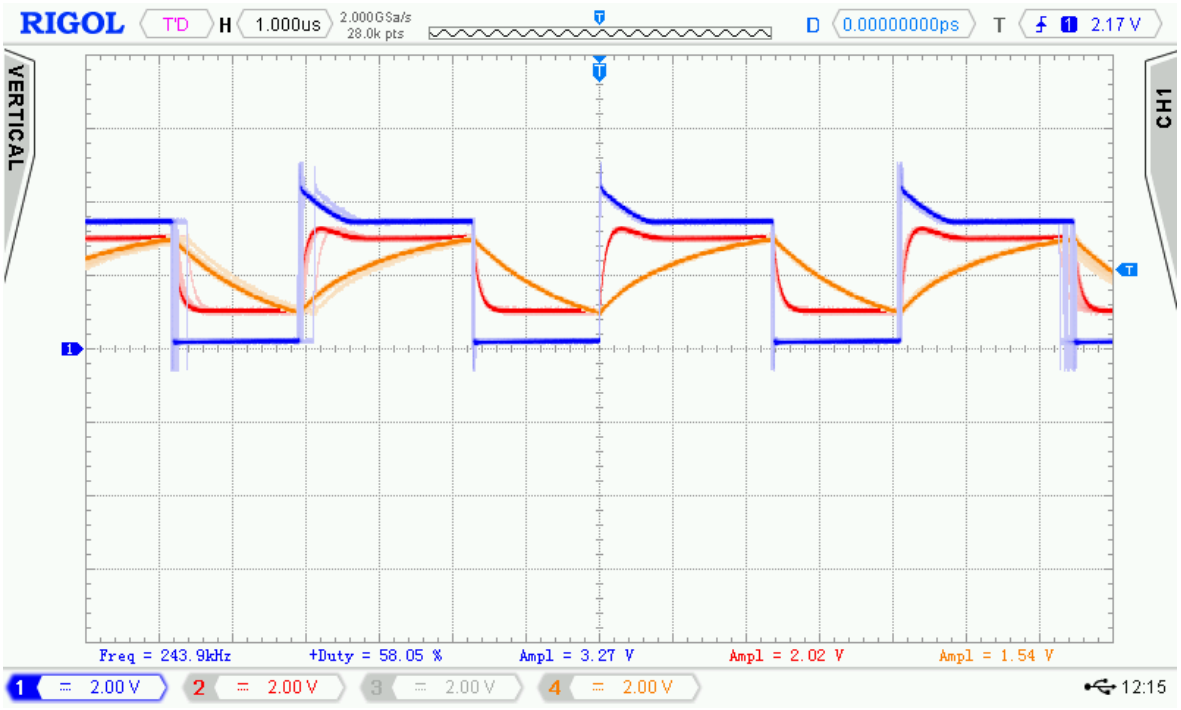

Figure 14: Oscilloscope image (output, inverting, non-inverting)

Step 2

The sawtooth signal from the inverting terminal is fed into step 2 of the regulator circuit (see figure 13, step 2). On the inverting terminal an adjustable voltage divider circuit is made from a resistor, R5 and a potentiometer. By adjusting the potentiometer, the duty cycle can be changed, as it is determined by when the constant voltage signal from the inverting terminal crosses the sawtooth signal from step 1, that is input at the non-inverting terminal. From this step a square output signal with the wanted duty cycle is at the output and can be fed into step 3.

Step 3

Step 2 will output a square signal with an amplitude of around 5 V, but as the MOSFET threshold voltage is 4 V [15], this will not be enough to drive it. An additional power supply of 9 V has been connected to power the gate driver, to boost the voltage of the output. The chosen gatedriver is UCC27322 [22], as it is easy to connect and meets the requirements. Figure 15 shows the output from step 3, and the signal that will be fed into the MOSFET.

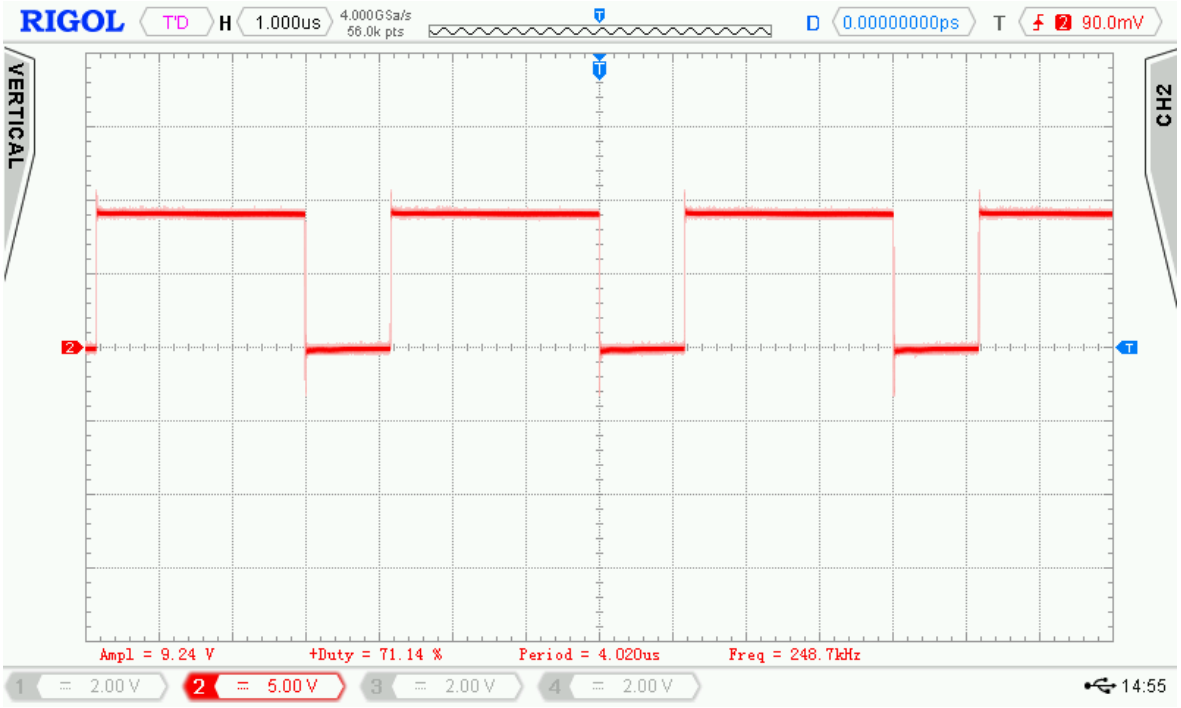

Figure 15: Oscilloscope image (output)

5.3 Assembling the circuit

On figure 4 in section 4.1 the schematic of a flyback converter is shown. Besides the coupled inductor, the IC and the MOSFET, the circuit consist of an input voltage source, a diode, an output capacitor and a load.

The input voltage source was in section 3 set to deliver 3.3 V, and 0.5 W.

The diode should have a breakdown voltage of 1 kV, whereas the RURP8100 diode has been chosen, as it was in stock and met the required breakdown voltage. [23] The diode has a forward voltage of 1.8 V, which is quite common for diodes. This will be slightly altered as the temperature changes, as it will in space. The recovery time is 100 ns which corresponds to 2 % of the period.

The output capacitor needs to be able to withstand a 1 kV voltage as well, whereas the 1206AA101JAT1A capacitor has been chosen. [24] It has a capacitance of 100 pF, which is very small, but no other capacitors at Farnell could withstand as high a voltage as this one. Two capacitors are connected in parallel to get a capacitance at 200 pF at the load, so it can store more charge.

The load size is determined from Ohm's Law, displayed in equation 5.26, to be 2 MΩ.

$$R = \frac{V}{I} = \frac{1.00\,\mathrm{kV}}{0.05\,\mathrm{mA}} = 2.00\,\mathrm{M\Omega} \tag{5.26}$$

The assembled circuit for the converter is found in the appendix on figure 21. Pictures of it is shown on figure 16.

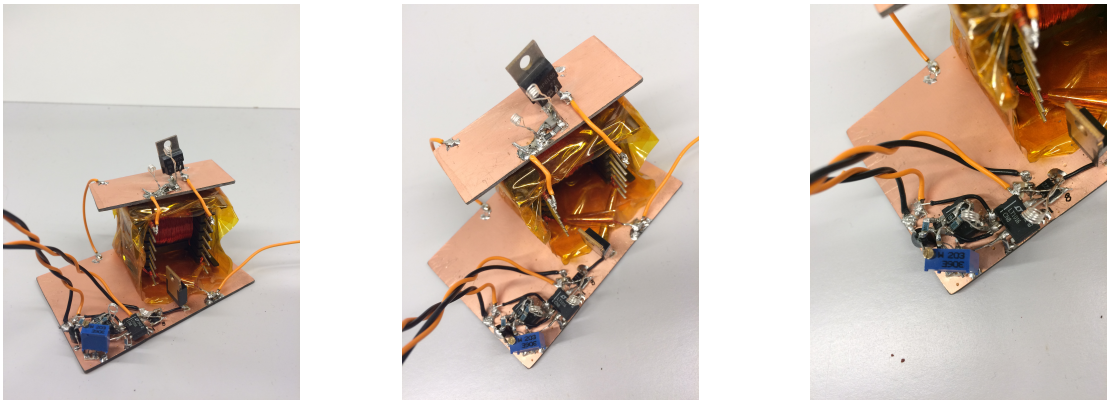

(a) View from front (b) View from top (c) Close-up of the switch circuit

Figure 16: Pictures of the assembled circuit

6 The pulse generator

Due to time constrictions no pulse generator has been realized yet.

The general idea of it is to use another switch and regulator circuit, possibly the AIM, to set the frequency and pulse length, as determined in section 3 and a capacitor where charge can be accumulated, which can then be discharges fast when the switch is on, and deliver the required output power of 1 kV. This system would be inserted where the load is in the flyback circuit (figure 21 in the appendix), in series with the thruster. Difficulties might arise with this as the frequency is so slow, so it can be complicated to construct the regulation.

7 Expected measurement results

Since the IC does not exist in LTspice, it must be replaced with a signal generator to run a circuit simulation, and analyze the different currents and voltages throughout the circuit. The simulation circuit is shown on figure 17. A various N-channel MOSFET has been chosen to run the simulation. The inductances are also chosen randomly, although the turns ratio is correct.

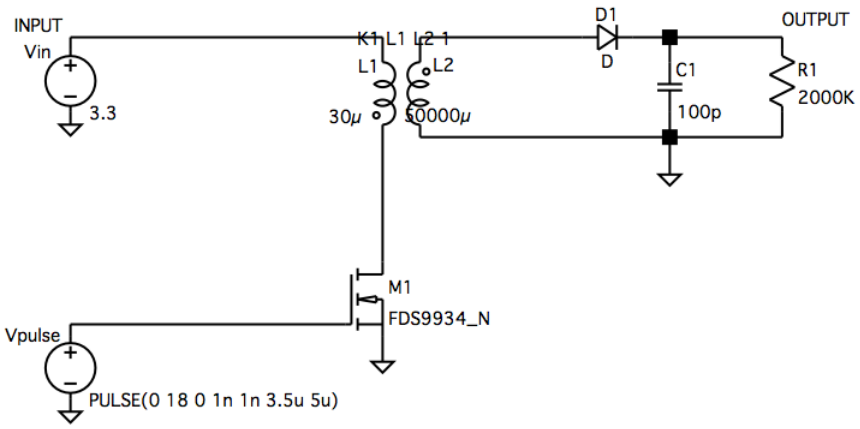

Figure 17: LTspice simulation circuit of the flyback converter

The figures on 18 are the result of the simulation.

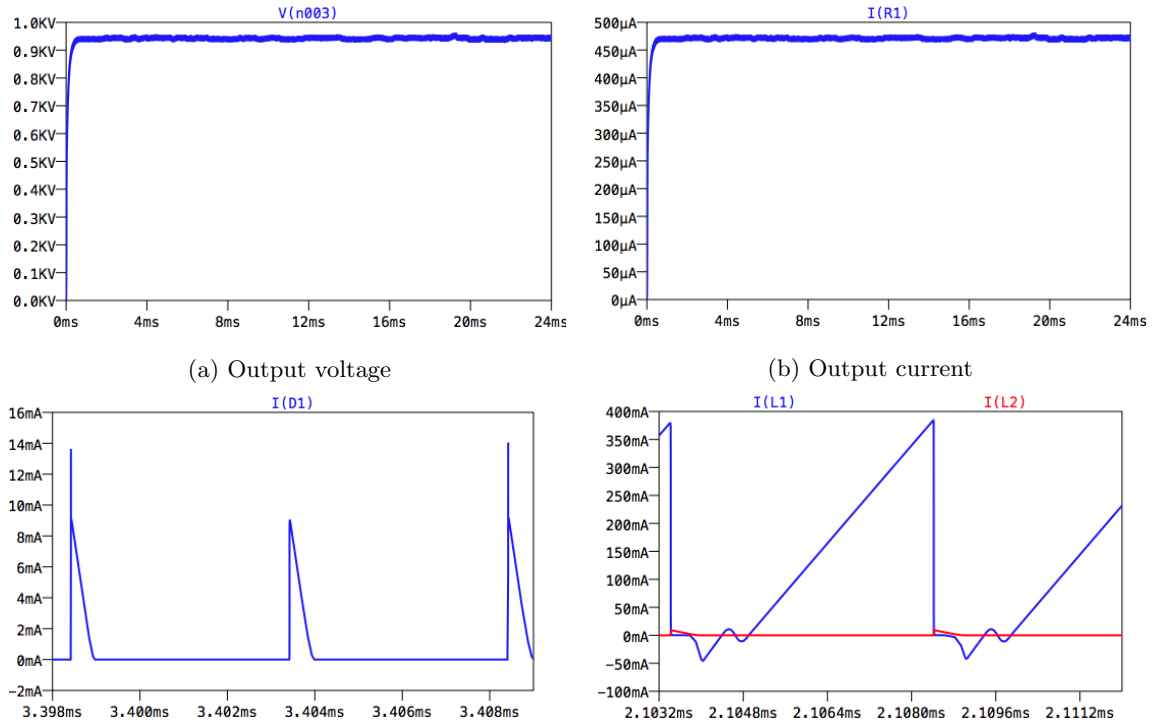

(a) Output voltage

(b) Output current

(c) Diode current

(d) Inductor currents (primary, secondary)

Figure 18: Simulation results

The output voltage on figure 18a rises fast, before it settles. The coupled inductor inductace values are the reason why it does not go all the way up to 1 kV, even though the turns ratio is correct. A small ripple is present in the output voltage, which can be difficult to avoid, although this would have been preferred.

Figure 18b shows the output current over the load resistor, R1. The current follows the same pattern as the voltage with the fast rise before it settles. A ripple is present here as well. The expected value was 500 μA, which it would have been if the voltage had been 1 kV, so this is due to the coupled inductors.

On figure 18c the diode current is shown. When the MOSFET switches to low, the diode starts conducting, until the coupled inductor is discharged.

The inductor currents are shown on figure 18d. During the MOSFET on time, the primary side is charging, and when the MOSFET switches to the off position, the secondary side discharges the accumulated charge from the coupled inductor out into the output of the circuit.

8 Measurement results

To acquire the measurement results, the voltage sources were connected to the circuit and the values pre-adjusted to the required circuit voltages. Three different sources were used to power the AIM, gate driver, and the rest of the circuit. The duty cycle was kept at 0 % by turning the potentiometer all the way counter clockwise, while the sources were connected and turned on. The duty cycle was then slowly turned up, while the voltages in the circuit were monitored, by turning the potentiometer clockwise.
The output from the oscilloscope at a 70 % duty cycle is shown on figure 19, where the statistics box on top, shows the output parameters. The gate signal from the AIM is as expected, with a pretty plane top. By the drain of the MOSFET the signal oscillates a lot in the beginning, due to a forced switch in the coupled inductor. Ideally the switch should be linear, and without the oscillations.

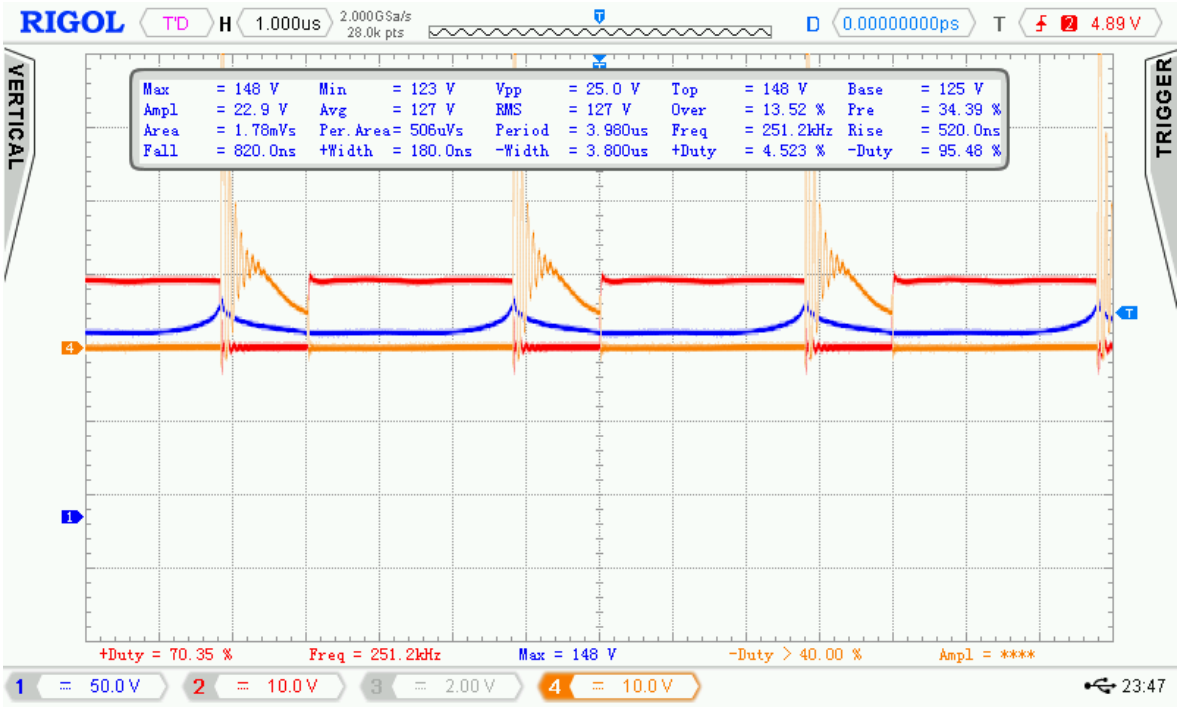

Figure 19: Oscilloscope image (output, gate signal, MOSFET drain signal)

The output signal is however very low compared to the expected 1 kV, with an amplitude of around 150 V. An additional capacitor was added to stabilize the output signal, and make it more of a DC than an AC signal. Supplementary capacitors may add to further leveling of the output.
Furthermore, almost 2 A was drawn at the 3.3 V source, which exceeds the calculated ideal value of 0.15 A by far.

9 Discussion and error detection

It is clear from the results in section 8 that the output voltage was not as much as was wanted. Furthermore if the output power over the load is calculated, this is close to 0 W, which will not be able to power a Hall Effect Thruster, nor a PPT.
Since the signal feeding into the MOSFET is at it was expected to be, the main errors must be found in the remaining part of the circuit. By further examination of the coupled inductor, two factors, which had been neglected in the design process, performs a major role in the power loss.

9.1 Coupling

Due to the large amount of windings on the secondary side of the coupled inductor, they must be layered to fit them all. Approximately 20-30 layers were made on the secondary side of the inductor, and if figure 20 is studied, the losses in the layers is extensive when it exceeds 10 layers. Due to this loss, the all layers after around layer 10 is not linked, and might as well not be there.

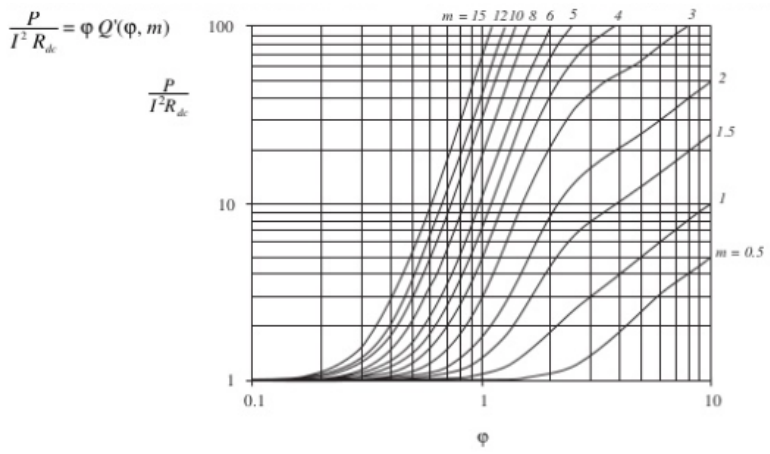

Figure 20: Diagram of the increased copper loss in layer [12]

To avoid this, a different type of inductor may be used. Instead of using a quadratic core, a rectangular core can add more window length, so fewer layers can be made. Otherwise they duty cycle can be adjusted further, to decrease the required turns ratio.

9.2 AC resistance

As the current cannot change momentarily in an inductor, resistance will occur whenever the MOSFET switches. Since the MOSFET in the built circuit switched 250 times every second, it is a lot of switches when many windings occur, as on the secondary side. Resistance is met at every switch, which when added up consumes a great amount of power.

9.3 Additional sources of error

The loop lengths around the circuit board will contribute with inductance as well, which will consume power. By looking at figure 16 one can see that the wires are kept as short as possible, however some of the loops are still big, which creates inductance.
As the circuit is constructed on copper plates, loose connections may occur, as the circuit is build in three dimensions to minimize the distances between the components.
Input impedance and inductance in the measurement equipment can cause small errors in the results, if they are of the same scale as the measured values. This has been seen to alter the results slightly.

10 Conclusion

With all the errors in the experiment it is very difficult to prove a flyback converter fit to power a Hall Effect thruster in space. Further development to increase the linkage and decrease the AC resistance must be made. A printed circuit board must be designed as well, before it is near ready to be sent into space.

Numerous tests on the circuit before launch must be made. These tests include a shake test, to check if the connections in the circuit are stable enough to survive the shaking during the launch of the rocket. A heat test, since the temperature in space varies a lot, so the circuit will have to be able to withstand both high and low temperatures, as it will experience as it orbits Earth. An ion tests to check stability in the circuit when solar radiation hits.
The DTU satellite project also provides the opportunity to test the electronics on a stratosphere balloon, where the conditions will be closer to the conditions in space than to the conditions in a laboratory. Further development on the converter during the next few months, will make it ready for a stratosphere balloon test in September.

Even though the output voltage and power was not near the wanted levels, the design still proved that it worked, by converting 3.3 V to 150 V.
This small success will not make it very far in a space race, or if asteroid mining should become a reality, but it is definitely a step along the way, towards the journey to the far universe.

References

[1] *What is the Hall Effect?*
Melexis, https://www.melexis.com/en/articles/hall-effect

[2] *Fundamentals of Electric Propulsion: Ion and Hall Thrusters*
Dan M. Goebel and Ira Katz, https://descanso.jpl.nasa.gov/SciTechBook/series1/Goebel__cmprsd_opt.pdf, March 2008

[3] *FIELD EMISSION ELECTRIC PROPULSION THRUSTER MODELING AND SIMULATION*
Anton Sivaram VanderWyst, http://ngpdlab.engin.umich.edu/files/papers/VanderWyst.pdf, 2006

[4] *Space Propulsion : Let's do it Better Electrically*
Richard S. Baty, http://www.au.af.mil/au/afri/aspj/airchronicles/aureview/1973/Nov-Dec/baty.html, October 2003

[5] *Pulsed Plasma Thrusters*
NASA, https://www.nasa.gov/centers/glenn/about/fs23grc.html, May 2008

[6] *Asteroid Mining*
Julie Søborg Dresler Petersen

[7] *Energy storage in capacitors*
John Hearfield, http://www.johnhearfield.com/Physics/Capacitor_energy.htm, 2010

[8] *ETD 34/17/11 : Core and accessories*
TDK, https://en.tdk.eu/tdk-en/529424/products/product-catalog/ferrites-and-accessories/epcos-ferrites-and-accessories/er-etd-eq-cores-and-accessories-, June 2013

[9] *Calculator for Skin Effect Depth*
Chemandy Electronics, http://chemandy.com/calculators/skin-effect-calculator.htm, February 2016

[10] *Copper Loss*
Centurion Energy, http://centurionenergy.net/energy-loss-of-a-wind-turbine/12, March 2013

[11] *Resistance and resistivity*
School Science, http://resources.schoolscience.co.uk/CDA/16plus/copelech2pg1.html

[12] *Fundamentals of Power Electronics*
Robert W. Erickson and Dragan Maksimovic, 2001

[13] *Primary Alkaline Manganese Cylindrical Battery*
http://www.varta-microbattery.com/applications/mb_data/documents/data_sheets/DS4122.PDF, May 2013

[14] *Power Electronics : A First Course*
Ned Mohan, November 2011

[15] *TrenchMOS transistor Standard level FET*
Philips Semiconductors, http://www.datasheetcatalog.com/datasheets_pdf/P/H/P/5/PHP55N03T.shtml, September 1997

[16] *100V Isolated Flyback Controller*
LT3748 IC from Linear Technology, http://cds.linear.com/docs/en/datasheet/3748fb.pdf, 2010

[17] *LT8309/LT3748 Demo Circuit - 60W, 12V Output, Isolated Telecom Supply (36-72V to 12V @ 5A)*
Linear Technology, http://www.linear.com/designtools/software/demo_circuits.php, March 2014

[18] *UC3842B: High Performance Current Mode Controllers*
ON Semiconductor, https://www.onsemi.com/pub/Collateral/UC3842B-D.PDF, September 2013

[19] *Towards Active Transducers*
Søren Poulsen, http://orbit.dtu.dk/en/publications/towards-active-transducers(ad86580b-cbf3-4ccf-9dfe-ae15ce1a8fdc).html, Dec 2004

[20] *LT1016 : UltraFast Precision 10ns Comparator*
Linear Technology, http://cds.linear.com/docs/en/datasheet/1016fc.pdf, 1991

[21] *LM336 : 2.5V Reference Diode*
Texas Instruments, http://www.ti.com/lit/ds/symlink/lm336-2.5-n.pdf, June 2005

[22] *Single 9-A High-Speed Low-Side Mosfet Driver With Enable*
Texas Instruments, http://www.ti.com/lit/ds/symlink/ucc27322.pdf, January 2016

[23] *RURP8100 8A, 1000V Ultrafast Diodes*
Fairchild Semiconductor, http://www.mouser.com/ds/2/149/RURP8100-1011998.pdf, 2001

[24] *1206AA101JAT1A : High Voltage MLC Chips For 600V to 5000V Applications*
AVX Corporation, http://www.farnell.com/datasheets/2237836.pdf?_ga=2.180674467.565173479.1496568171-338825097.1488546401, December 2016

All website sources were last visited on 08/06-17

Appendix

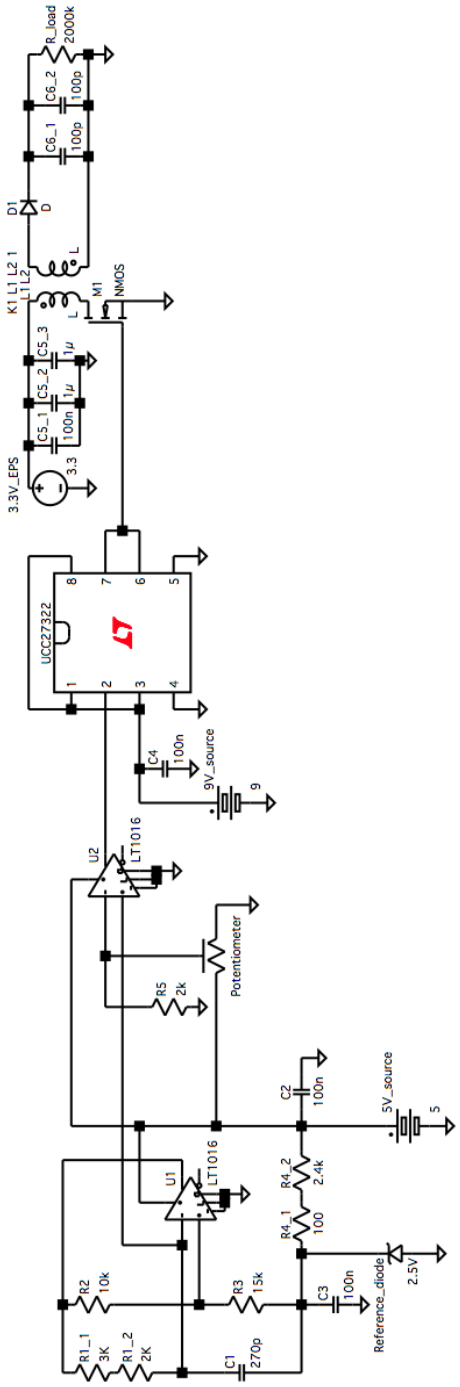

Figure 21: Schematic of the full flyback circuit

DTU Space
National Space Institute
Technical University of Denmark

Elektrovej bygning 328
2800 Kgs. Lyngby
Tlf. (+45) 4525 9500
Fax (+45) 4525 9575

www.space.dtu.dk